LAWRENCE
LIVERMORE
NATIONAL
LABORATORY

LLNL-CONF-404224

Spatial structure of scrape-off-layer filaments near the midplane and X-point regions of Alcator C-Mod

J. L. Terry, S. J. Zweben, M. V. Umansky, I. Cziegler, O. Grulke, B. LaBombard, D. P. Stotler

May 28, 2008

18th Conference on Plasma Surface Interactions
Toledo, Spain
May 26, 2008 through May 30, 2008

Disclaimer

Spatial structure of scrape-off-layer filaments near the midplane and X-point regions of Alcator C-Mod

J.L. Terry [a*], S.J. Zweben [b], M.V. Umansky [c], I. Cziegler [a], O. Grulke [d], B. LaBombard [a], D.P. Stotler [b],

[a] *Plasma Science and Fusion Center, MIT, Cambridge, MA, USA 02139*

[b] *Princeton Plasma Physics Laboratory, Princeton, NJ, USA 08543*

[c] *Lawrence Livermore National Laboratory, Livermore, CA, USA 94550*

[d] *Max Planck Institute for Plasma Physics, Greifswald, Germany*

Abstract

Movies of edge turbulence at both the outboard midplane and the region outboard of the typical lower X-point location in C-Mod have been obtained using Gas-Puff-Imaging together with fast-framing cameras. Intermittent turbulent structures, typically referred to as blobs or filaments, are observed in both locations. Near the midplane the filaments are roughly circular in cross-section, while in the X-point region they are highly elongated. Filament velocities in this region are ~3x faster than the radial velocities at the midplane, in a direction roughly normal to the local flux surfaces. The observations are consistent with the picture that the filaments arise in outboard region and, as a consequence of the rapid parallel diffusion of the potential perturbations, map along field lines. A simulation using the 3D BOUT turbulence code has been made, with the result that reproduces many of the spatial features observed in the experiment.

PSI18 Keywords: Cross-field Transport, Intermittent Transport, Edge Plasma, Alcator-C-Mod, Visible Imaging

JNM Keywords: Plasma Properties

PACS: 52.35.Ra, 52.30.-q, 52.55.-Fa, 52.70.Kz

*Corresponding Author Address: 175 Albany St., Cambridge, MA 02319 USA

*Corresponding Author E-mail: terry@psfc.mit.edu

Presenting Author: James L. Terry

Presenting Author E-mail: terry@psfc.mit.edu

I. Introduction

There is great interest, both experimental and theoretical, in the intermittent convective transport that is routinely observed in the far scrape-off-layer (SOL) on the outboard "bad-curvature" side of the tokamak plasmas. In the literature this is typically referred to as transport due to blobs or filaments or mesoscale structures, all names for the same phenomenon. It dominates the perpendicular particle transport there [[1]]. The interest in it derives primarily from its impact on crucial reactor issues like density-scale-length in the far-SOL, divertor design, wall-recycling, and the physics of the density limit. Most previous experimental studies have measured characteristics of this transport phenomenon in the outboard midplane region. It is the purpose of this work to present and discuss some of the characteristics of blobs/filaments in regions away from the outboard midplane, in particular, in the region outboard of the lower X-point, and to relate them to blob characteristics in the midplane region. Our choice to view the X-point region was made primarily for two reasons: we wanted to get as close as was practical to the X-point in order to investigate the effects on the filaments (if any) of the flux expansion and magnetic shearing that occurs when moving (along field lines) to the X-point region, and we wanted to be able to distinguish whether the filaments motion there was normal to the local flux surfaces or was in the major radial direction, something that the same in the midplane region.

II. Experimental Details

For and prior to this study, turbulence imaging diagnostics on C-Mod viewed both the outboard and inboard midplane regions (Fig. 1). The outboard region is viewed (approximately parallel to the field) using a 2D fast-framing camera [[2]]. Also within the same view there are two linear arrays of views, one radial and the other vertical, that are coupled to

filtered photodiodes, which are sampled at a 1MHz rate. Viewing the inboard midplane region is another radial array of views. These views are close to gas puff nozzles that provide a toroidally-localized source of deuterium whose D_α emissions respond to local n_e and T_e fluctuations and are detected by the optical diagnostics (so-called Gas-Puff-Imaging (GPI) [3]). These nozzles are typically ~1-3 cm from the local separatrix and at the edges of the views themselves. To complement these diagnostics, we installed a new view of the region just outboard of the location of the typical lower X-point for the reasons stated above. (For brevity we will hereafter refer to this as the "Xpt view" or the "Xpt region", even though it does not actually view the X-point.) This ~6 x 6 cm view is also approximately along the local field. A nozzle embedded in the divertor structure under the view provides the local gas puff. This nozzle is ~ 3 cm below the bottom of the view, ~6 cm from the view center, and ~7-9 cm below the typical separatrix location. The view is separated toroidally from the viewed outboard midplane region, and the two regions are not connected magnetically. All views are shown in Fig. 1. Movies of edge turbulence in "Xpt region" and at the midplane are obtained using fast-framing (150,000 frame/s) cameras [4]. While, for this study, movies from both views were not recorded simultaneously, the outboard midplane "diode-views" were recorded simultaneously with the movies at each location. For analysis of the images of the "Xpt region", plasmas in DN, USN, or limited configuration were used, since in those configurations emission from the local puff was much greater than the intrinsic D_α emission (as is necessary in order to localize the measurement).

III. Comparisons of filament characteristics - outboard midplane vs "Xpt region"

As has been previously reported [see ref [5] and references therein], turbulence in the outboard far-SOL of C-Mod and most other tokamaks is intermittent. Distributions in the fluctuation magnitudes of various measured quantities (like local GPI emission, I_{sat}, and V_{float}) are

strongly skewed toward larger magnitude fluctuations. Imaging at the outboard midplane in the vertical-toroidal plane shows that the turbulent fluctuations have a filamentary structure, aligned with the local field and with $k_{\|} << k_{perp}$[e.g. [6,7]]. When these filaments are viewed in a vertical-radial plane at the midplane, along chords parallel to the local field, they appear as "blobs" that are roughly circular in shape with a characteristic diameter (correlation length) of ~1 cm [[8]]. Images from the outboard midplane view illustrating this can be found in ref [[9]]. The blobs there move both radially and poloidally with typical radial speeds of ~500 m/s [[10]]. Fluctuations at the inboard midplane are much reduced, both in absolute and relative magnitude [[9,11]]. Blobs are not observed there.

Imaging at the "Xpt region" also shows intermittent fluctuations. Their cross-sectional shape as imaged with GPI, however, is much different than that at the midplane. Highly-elongated "fingers" are observed, as illustrated in a single frame from this view and shown in Figure 2. In the lower left part of the view, the long dimension of the fingers is typically tilted by angles of up to ~45° below horizontal. Motions of the fingers there are primarily outward across flux surfaces (i.e., approximately perpendicular to the separatrix, also shown in Fig. 2) with speeds ~3x the radial speeds of the midplane blobs (as determined by the time-delay cross correlation method described in [[10]]). In the upper right part of the view, the finger axes are typically close to horizontal. Analyses of the "Xpt region" movies and of the simultaneously-measured outboard midplane "diode view" time-signals yield profiles of auto-correlation times for the fluctuations, $\tau_{auto}(\rho)$, that are the same (within the scatter). (ρ is the distance outside the separatrix when mapped to the outboard midplane.) For DN discharges τ_{auto} is typically ~30 μs just inside the separatrix, falling to 15-20 μs at ρ >/~1.5 cm. Thus the auto-correlation times of the fluctuations, due mostly to the filament motion, are approximately the same in both regions.

The observations described above are reconciled within the following physical picture: Filaments of high density plasma are generated primarily in the outboard, bad-curvature region. This is directly or indirectly related to the strong ballooning-like particle transport implied by other measurements, e.g. the observed SOL flows [12] and consistent with the relatively small level of turbulence at the inboard midplane. Following the basic model for filament motion [13]: Since the parallel conductivity of the plasma is large, the electrostatic potentials set up from curvature and BxgradB drifts are transmitted along the field diffusively by a competition between parallel and cross-field currents. The filament is thus polarized in a way that depends upon the integration of the gradient of the cross-field current along the field. A parallel diffusion coefficient for potential fluctuations, $D_\phi \sim \sigma_\parallel 4\pi V^2_{alfven}/(c^2 k_{perp}^2)$, can be derived from either the continuity or vorticity equation. This implies that any potential perturbation will be communicated between the midplane and "Xpt" regions in C-Mod on a fast time scale of ~1 μs (for B_t=4T, n_e=3x10^{20} m^{-3}, T_e=25 eV, k_{perp}=0.06 m^{-1}, $\lambda_\parallel$=3 m). It is to be compared to the timescale for transport of *density* perturbations along the field between midplane and "Xpt" regions of $\lambda_\parallel/C_s$ ~100 μs. Similarity of the measured profiles of auto-correlation times is consistent with a fast (</~10 μs) timescale for propagation. Thus we expect that the rapid parallel propagation of potential gives rise to field-aligned filaments whose large scale ($k_{perp}\rho_s$~0.1) features map along field lines and whose drive and damping responses are integrated over the field line length. Previous cross-correlation measurements on C-Mod [7], for which a midplane "diode view" was approximately connected magnetically to a scanning *probe* that sampled the same poloidal region as the "Xpt view" (but at a different toroidal angle) are also consistent with this picture in that 1) parallel correlation of density fluctuations was observed and 2) the measured dipole structure of potential

fluctuations in the "Xpt region" was consistent with the measured size and outward propagation of the density fluctuations at the midplane.

This picture thus predicts that large scale cross-field features of the filaments should magnetically map between the midplane region and the "X-pt region". Indeed, *circular structures at the midplane (i.e. the blobs) do map into structures in the "Xpt region" that are highly elongated and tilted (i.e. the fingers), as observed.* We have performed this mapping in detail for specific shots. Flux tubes that are circular (1 cm diam.) in cross-section at the midplane i.e. the rough size and shape of the filament cross-sections observed in the midplane region, are mapped to the "Xpt view", where they are approximately ellipsoidal in cross-section, having been stretched by flux expansion and tilted by shearing. We have quantitatively compared the tilts of these mapped flux tubes with the tilts of the observed fingers and the lengths of the major diameters of the mapped flux tubes with the correlation lengths of the fluctuations along the finger tilt axes. The observed tilt angles are determined by finding (at any point in the image) the angle of the line for which the line-integrated cross-correlation of the reference location and the rest of the image is maximum. The correlation length along this line is then calculated. Typically ~300 sequential images are used for these determinations. Results from such a comparison are shown in Figure 3, where the black arrows represent the lengths and tilts of the major axes of the 1-cm-mapped-flux-tubes. The angles of red arrows represent the *measured* tilt angles, while the lengths of the red arrows are proportional to the *measured* correlation lengths, determined as described above. There is typically excellent agreement in the tilt angles in the lower left section of the experimental view. The measured finger correlation lengths there are within a factor of 2 of the flux tube major diameters, also in good agreement, given the quantities being compared.

However, a major and obvious inconsistency between the flux-tube-mapping model and the observations is the disagreement between finger tilts and finger lengths observed in the entire upper portion of the images and those predicted by the mapping model. The fingers in the upper portion of the view are typically nearly horizontal and 2-5 cm in length, while the mapping predicts tilts of -10° to -35° with flux tube major diameters of ~1.6 cm. We attribute this discrepancy to a limitation in the gas-puff-imaging. As mentioned in Section II, the toroidal extent of the puff defines the toroidal localization of the emission forming the image. For imaging in the "Xpt region", the nozzle is significantly further from the view than for the midplane views, resulting in a significantly larger gas cloud at the view location. Indeed, modeling of the puff and view with the 3D neutrals code DEGAS2 [14] indicates that the toroidal FWHM of the emission from the puff is ~10 cm at the center of the view, increasing to 15-20 cm at the top of the view. Since the lines-of-sight are in the same planes as the local field, emission along the length of a single field line will appear in the image as a nearly horizontal line. Modeling of this effect shows that emission from a small cross-section of filament extending toroidally for 20 cm along a field line will be imaged as a horizontal "finger" of ~2 cm length in the top of the view. When this effect is convolved over the entire cross-section expected for the filament from magnetic mapping, then correlation lengths that are longer and at much less tilted angles than the mapped filament cross-sections will result. Since the measured correlation lengths in the upper part of the view are 2-5 cm and nearly horizontal, it is probable this effect is playing a significant role in the observations and may be the primary reason for the disagreement with the mapping there. (The extent of the cloud in the lower part of the view is 5 cm, yielding a horizontal component to the finger images there, due to this effect, of only 0.3 cm.)

The flux-tube-mapping model also predicts that the cross-field velocities should be roughly normal to the local flux surface and related as the radial flux expansion ratio between the two viewed regions since the cross field dimension will be reduced by approximately the same ratio, thereby increasing E_{perp} in the E_{perp}xB drive, Quantitatively, velocities normal to the flux surfaces in the "Xpt region" that are ~3x faster than the midplane radial velocity are expected, roughly what we observe. This result has not been tested more quantitatively since simultaneous imaging of the same flux tube at the two locations has not been done. Finally we note that some aspects of the flux tube mapping of filaments have been discussed by Ryutov [15] before knowledge of these experimental results.

IV. Comparisons with Turbulence Simulation Results

Aspects of the spatial structure of the filamentary SOL turbulence have been examined using the BOUT 3D non-linear simulation code [16]. BOUT uses a system of reduced Braginskii fluid equations in realistic flux tube geometry, including X-point effects. For this simulation, turbulence in a flux tube domain (whose cross-section at the outboard midplane is 2 cm radially x 4 cm poloidally) is simulated for a C-Mod EFIT equilibrium with measured SOL profiles of n_e and T_e. Filaments of approximately the same size scale as in the experiments, i.e. features of ~1 cm size, appear at the midplane, although more fine scale structure is present in the simulation than is resolved in the experiment. Since the "Xpt view" of the experiment is much larger than a single poloidal cut of the simulation flux tube at this location, the toriodal periodicity in the simulation is used to fill the viewed region by mapping multiple poloidal cuts to a single plane at constant toriodal angle. This results in different cuts of the same filament appearing in each frame of the simulation realization, as seen in Fig. 4a, where the fluctuation ion density in the "Xpt view" is shown. It is clear that in this region the simulation filaments are tilted and elongated fingers. Using the same

analysis techniques that were used to determine the finger tilt angles for the experimental images, tilt angles for the simulation fingers were determined. As was done for the comparison with experimental tilt angles in Fig. 3, the simulation tilt angles (red arrows) were compared with those of elongated flux tubes that map from circles at the midplane (black arrows). The result is shown in Fig. 4b, where the angles are seen to be essentially the same. This indicates that the flux tube mapping of features with $k_{perp}\rho_s \sim 0.1$ is also observed in the BOUT simulation.

V. Discussion and Summary

We have studied the spatial structure and the parallel dynamics of the plasma blobs/filaments that appear routinely in the far SOL of Alcator C-Mod plasmas and are responsible for the bulk of the particle transport there. By imaging these filaments in the outboard midplane region and in the region of outboard of the lower X-point, we find that the roughly circular blobs at the midplane appear as elongated fingers in the "Xpt region". The elongated and sheared cross-sections of the filaments observed in the lower part of the "Xpt view" are quantitatively consistent with a magnetic mapping of roughly circular cross-sectioned structures at the midplane region. These features are also reproduced in a simulation using the BOUT turbulence code. Furthermore, the fingers in the lower part of the "Xpt view" move outward approximately normal to flux surfaces with speed roughly 3x the outward radial velocities observed near the midplane. Thus we have provided measurements of the cross-sectional shapes of the filaments and their cross-field dynamics at two locations and discussed a model that can explain many of the observed features. In the model, rapid parallel diffusion of potential perturbations results in the magnetic mapping (at least) of large ($k_{perp}\rho_s \sim 0.1$) filamentary structures. Such a mapping is quantitatively consistent with the observations. Results consistent with these, as well as similar conclusions, have also been published in ref [6], in which probe measurements of SOL fluctuations in W7-AS stellarator

plasmas were analyzed.

There are a number of implications from this picture both for transport in the main chamber and for transport and dynamics in the divertor. Continued magnetic shearing and flux expansion close to the X-point may have important consequences for parallel and perpendicular transport, both because of their effects on the stability of the filament and because, if the mapping continues to hold, the filaments are deformed into shapes where the poloidal scale length approaches the ion gyro-radius [17]. Whether the filaments cross the X-point region into the divertor is still unknown. If they do or if they arise in the divertor plasma, there exist possibilities for manipulating them and their effects on the divertor plasma, as discussed in detail in refs [18,17].

Acknowledgement

We would like to acknowledge valuable discussions with D. Ryutov and R. Cohen of Lawrence Livermore Laboratory and T. Stoltzfus-Dueck and J. Kommes of PPPL. This work is supported by DoE Coop. Agreement DE-FC02-99-ER54512 (MIT) and Contract No. DE-AC02-76CHO3073 (PPPL) and Contract DE-AC52-07NA27344 (LLNL).

Figure Captions

Figure. 1 – Poloidal X-section of a DN C-Mod discharge, showing the turbulence imaging diagnostics: the 2D"Xpt view", outboard of the lower X-pt (red square); the 2D view at the outboard midplane (red square) with the radial and vertical arrays of diode-coupled views (red dots); and the radial array of views at the inboard midplane (red dots). For the GPI, gas is puffed from the 3 nozzles (purple).

Figure 2. A single movie image (2 μs exposure) from the"Xpt view" of a DN plasma showing the cross-sections of typical SOL filaments. The separatrix is also shown (blue). The gas is puffed from below the image.

Figure 3. Comparison between measured finger tilts and lengths and those predicted by mapping 1 cm diam. flux tubes from the midplane to the viewing location. The angles for which the line integral cross-correlation values in the movie images are maximum are shown by the red arrows, whose lengths are proportional to the fluctuation correlation lengths along that line. The angles and lengths of the major axes of the mapped flux tubes are shown by the black arrows. The actual correlation lengths and major diameters are 2.86x longer than shown, but are scaled in the figure for clarity.

Figure 4. (a) The ion density fluctuation at one instant within the "Xpt region" from the BOUT simulation, showing multiple poloidal cuts of a typical filament (see text). (b) Comparison of the tilt angles of the filament fingers of the simulation (red arrows) and the tilt angles of the major axes of the mapped flux tubes (black arrows). The lengths of the simulation fingers were not found, since the correlation lengths along the tilt angles extended outside the simulation domain. Thus all of the red arrows are the same length. The lengths of the black arrows are proportional to the lengths of flux tube major axes.

References

[1]L. Rudakov, J.A. Boedo, R.A. Moyer et al., Plasma Physics and Controlled Fusion IAEA Technical Committee Meeting on Divertor Concepts, 11-14 Sept. 2001 44, 717 (2002).
[2]J L Terry, S. Zweben, B. Bose et al., Review of Scientific Instruments 75, 4196 (2004).
[3]J. L. Terry, R. Maqueda, C. S. Pitcher et al., Elsevier. Journal of Nuclear Materials 290, 757 (2001).
[4]A Phantom v7.3 camera; www.visionresearch.com.
[5]S. J. Zweben, J. A. Boedo, O. Grulke et al., Plasma Physics and Controlled Fusion 49, 1 (2007).
[6]J. Bleuel, M. Endler, H. Niedermeyer et al., New Journal of Physics 4, 38.1 (2002).
[7]O. Grulke, J L Terry, B LaBombard et al., Physics of Plasmas 13, 012306 (2006).
[8]S. J. Zweben, D. P. Stotler, J. L. Terry et al., Physics of Plasmas 9, 1981 (2002).
[9]J. L. Terry, S. J. Zweben, K. Hallatschek et al., Physics of Plasmas 10, 1739 (2003).
[10]J.L. Terry, S.J. Zweben, O. Grulke et al., Journal of Nuclear Materials 337-339, 322 (2005).
[11]B. LaBombard, J.E. Rice, A.E. Hubbard et al., Nuclear Fusion 44, 1047 (2004).
[12]B. LaBombard, J. E. Rice, A. E. Hubbard et al., Physics of Plasmas 12, 056111 (2005).
[13]S. I. Krasheninnikov, Physics Letters A 283, 368 (2001).
[14]D. P. Stotler, C. S. Pitcher, C. J. Boswell et al., Journal of Nuclear Materials 290-293, 967 (2001).
[15]D. D. Ryutov, Physics of Plasmas 13, 122307 (2006).
[16]X. Q. Xu, R. H. Cohen, G. D. Porter et al., Nuclear Fusion 40, 731 (2000).
[17]D. Ryutov and R.H. Cohen, to be published in Contrib. to Plasma Phys. 48 (2008).
[18]R. H. Cohen, B. LaBombard, D. D. Ryutov et al., Nuclear Fusion 47, 612 (2007).

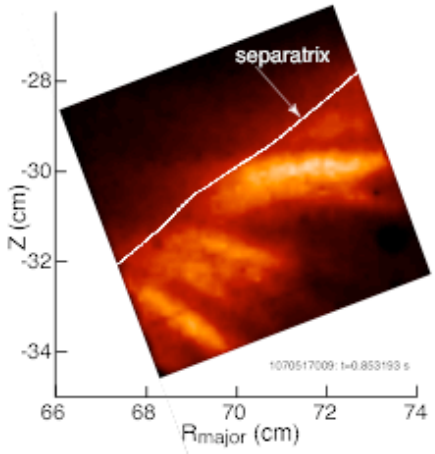

Figure 2 - Terry, et al (O-22)
75 mm width
79.6 mm height

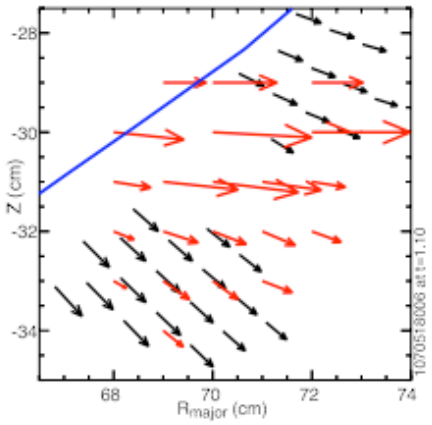

Figure 3 - Terry, et al (O-22)

70.0 mm height (when width is scaled to 75 mm)

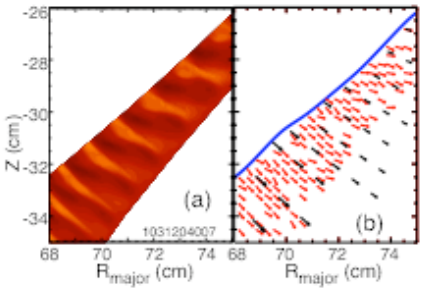

Figure 4 - Terry, et al (O-22)
75 mm width
52.5 mm height